RSC Advances

PAPER

View Article Online
View Journal | View Issue

Cite this: *RSC Adv.*, 2020, **10**, 15614

A PANI-Fe_3O_4@ZnO nanocomposite: a magnetically separable and applicable catalyst for the synthesis of chromeno-pyrido[*d*]pyrimidine derivatives†

Fatemeh Chaghari-Farahani, Shahrzad Abdolmohammadi * and Reza Kia-Kojoori

Received 1st March 2020
Accepted 31st March 2020

DOI: 10.1039/d0ra01978j

rsc.li/rsc-advances

We report herein green, practical, PANI-Fe_3O_4@ZnO-nanocomposite-catalyzed cyclocondensation reactions involving 4-aminocoumarin, 1,3-dimethylbarbituric acid, and aromatic aldehydes in an aqueous medium at room temperature to synthesize 9,11-dimethyl-7-aryl-6*H*-chromeno[3′,4′:5,6]pyrido[2,3-*d*]pyrimidine-6,8,10(9*H*,11*H*)triones. This research aims to provide an applicable and high-yield protocol that follows the principles of green chemistry, with the use of water as an environmentally benign medium and the PANI-Fe_3O_4@ZnO nanocomposite as a magnetically recoverable catalyst.

1. Introduction

Current questions about the use and benefits of continuous flow chemistry,[1] including the elaborate design and development of sequences for the synthesis of alternative structurally complex molecules with structural diversity and eco-congeniality, are of great interest to organic chemists.[2] The use of multicomponent reactions (MCRs),[3] which involve important contributions resulting from the combination of a minimum of three reactants (or a reactant with three reaction centers) in a single step to form a product that incorporates frameworks containing substantial elements from all the reactants,[4,5] is a well-recognized tool in macrocyclization strategies, peptide cyclization, and the diversity-oriented derivatization of complex fused heterocycles.[6–15]

Magnetic nanoparticles (MNPs) have been attracted significant attention due to their wide range of various usages, such as in cancer treatment,[16] drug release,[17] and the simplification of catalyst separation. MNP-supported catalysts have also been extensively used in organic transformations.[18–23] Recent intensive developments in the field of supported nanomaterials have mainly focused on polymer-bound nanostructures due to their essential applications in photocatalysis,[24,25] superhydrophobic materials,[26] organic conductors, electromagnetic interference shielding, *etc.*[27] Polyaniline (PANI) is a highly promising polymer for developing novel catalyst supports owing to its energy band gap of 2.8 eV,[28] good stability, corrosion protection, non-toxicity, great intrinsic redox potential, and facile and low-cost synthesis.[29] The chromene nucleus is a well-known scaffold and an important feature of diverse natural products and medicinal agents.[30] Compounds carrying the chromene motif have been reported to possess diverse biological properties, such as antibacterial,[31,32] antimicrobial,[33–36] antioxidant,[37,38] antivascular, antitumor,[39] hypotensive,[40] anticancer,[41–44] local anesthetic, and antiarrhythmic activities.[45] Additionally, some chromene-bearing compounds have been previously found to have neurogenic and cognition-enhancing activities.[46] Pyridine is a nitrogen-containing basic heterocycle found in various synthetic and naturally occurring compounds that have been shown to possess promising agrochemical and pharmaceutical properties.[47]

As a part of ongoing studies into the synthesis of biologically significant heterocycles catalyzed by various inorganic nano-sized materials,[48–50] we explored a low-cost and ecofriendly cyclocondensation reaction for the synthesis of 9,11-dimethyl-7-aryl-6*H*-chromeno[3′,4′:5,6]pyrido[2,3-*d*]pyrimidine-6,8,10(9*H*,11*H*)trione derivatives in the presence of water as a green solvent and a PANI-Fe_3O_4@ZnO nanocomposite as a applicable heterogeneous catalyst at room temperature. The synthetic pathway is presented in Scheme 1.

2. Experimental

2.1. Materials and methods

All of the chemical materials used in this work were purchased from Merck and Fluka and were used without further purification. Melting points were determined using Electrothermal 9100 apparatus. IR spectra were obtained using an ABB FT-IR (FTLA 2000) spectrometer. ^{1}H NMR and ^{13}C NMR spectra were recorded using a Bruker DRX-500 AVANCE spectrometer at 500 and 125 MHz, respectively, using TMS as an internal standard

Department of Chemistry, East Tehran Branch, Islamic Azad University, P. O. Box 18735-138, Tehran, Iran. E-mail: s.abdolmohamadi@iauet.ac.ir; s.abdolmohamadi@yahoo.com; Fax: +98-21-3358 4011; Tel: +98-21-3359 4950

† Electronic supplementary information (ESI) available. See DOI: 10.1039/d0ra01978j

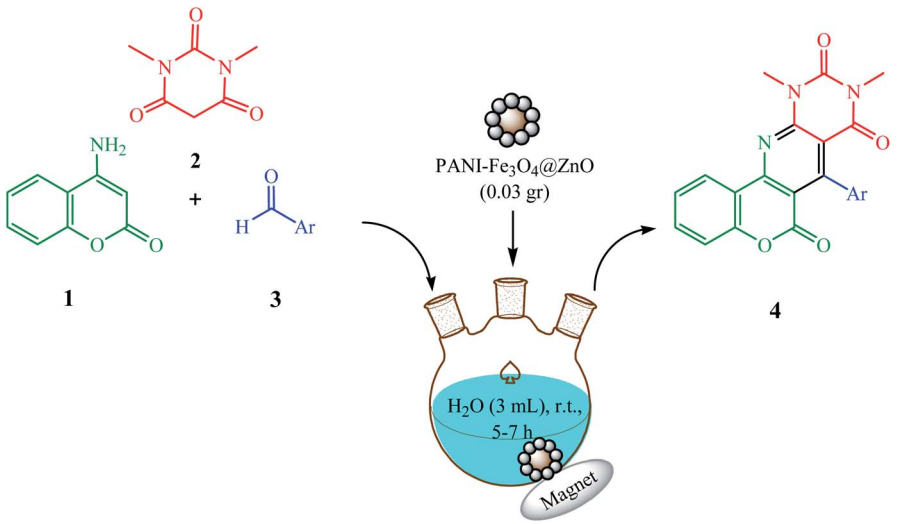

Scheme 1 The synthesis of 9,11-dimethyl-7-aryl-6*H*-chromeno[3′,4′:5,6]pyrido[2,3-*d*]pyrimidine-6,8,10(9*H*,11*H*)trione derivatives.

and DMSO-d_6 as a solvent. Elemental analyses were carried out using Foss-Heraeus CHN–O-rapid analyzer instruments. Powder X-ray diffraction data were obtained with a Rigaku D-max C III X-ray diffractometer using Cu Kα radiation ($\lambda = 1.54$ Å). The microscopic morphology of the catalyst was revealed using a scanning electron microscope (SEM, Philips, XL-30) equipped with energy dispersive X-ray analysis (EDX) apparatus. The microscopic morphology of the catalyst was studied using transmission electron microscopy (TEM) techniques on a Philips CM300 microscope operating with a 100 kV electron beam accelerating voltage.

2.2. Preparation of Fe_3O_4 nanoparticles

Fe_3O_4 magnetic nanoparticles (Fe_3O_4 MNPs) were prepared under solvothermal conditions. Firstly, a mixture of iron(III) chloride (0.6 g), ammonia (7 mL), and glycerol (25 mL) was magnetically stirred at 20 °C for 15 min. A reaction mixture color change from orange to deep brown occurred. Then, the resultant mixture was irradiated ultrasonically for 10 min. Then, the mixture was removed from the ultrasonic bath and magnetically stirred for 30 min. The obtained brown suspension was then placed into an autoclave and heated at 185 °C for 8 h. Then, the autoclave was cooled down gradually to room temperature. The synthesized Fe_3O_4 MNPs were separated using an external magnet, washed several times with distilled water, and dried under an air atmosphere for two days.

2.3. Preparation of the Fe_3O_4–ZnO nanocomposite

The synthesis of a core–shell nanostructured Fe_3O_4–ZnO nanocomposite with an iron oxide (Fe_3O_4) core and zinc oxide (ZnO) shell was carried out *via* a solvothermal process. First, a precursor solution was obtained from dissolving 4 g of Fe_3O_4 MNPs in 50 mL of distilled water, and this was magnetically stirred at room temperature for 20 min. Next, a mixture of polyvinyl pyrrolidone (PVP) (0.5 g), urea (3.8 g), and zinc nitrate (3 g) was added to the above solution under strong magnetic stirring. The obtained mixture was magnetically stirred at 90 °C for 1 h. The produced dark brown composite was then separated using an external magnet, washed with distilled water and ethanol several times, and dried in an oven at 80 °C for one day. The Fe_3O_4–ZnO nanocomposite powder was finally calcined for 2 h at 500 °C with a heating rate of 10 °C min^{-1}.

2.4. Preparation of the PANI-Fe_3O_4@ZnO nanocomposite

The as-prepared Fe_3O_4–ZnO nanocomposite powder (1 g) was added to 30 mL of 1 M HCl, and this was magnetically stirred at room temperature for 30 min. To the above suspension, 3 mL of aniline, 15 mL of 1 M HCl, and a solution of ammonium persulfate (APS) (0.03 g) in distilled water (15 mL) were then added dropwise at 5 °C, respectively. Then, the resultant mixture was magnetically stirred at room temperature for 5 h. The PANI-Fe_3O_4@ZnO nanocomposite was collected as a black precipitate using an external magnet, washed with distilled water and ethanol several times, and finally dried in an oven at 60 °C for one day.

2.5. General procedure for the synthesis of compounds 4a–h

A mixture of 4-aminocoumarin (**1**, 1 mmol), 1,3-dimethylbarbituric acid (**2**, 1 mmol), aromatic aldehyde **3** (1 mmol), and the PANI-Fe_3O_4@ZnO nanocomposite (0.03 g) in H_2O (3 mL) was stirred at ambient temperature for 5–7 h (see Table 2). After the completion of the reaction, as indicated *via* TLC (ethyl acetate : petroleum ether = 3 : 1), the catalyst was recovered simply from the reaction mixture using an external magnet. For reuse, the catalyst was washed with EtOH and dried in air at ambient temperature for several hours. Then the resultant mixture was filtered and the collected solid was dissolved in 5 mL of hot ethanol. The pure product was obtained *via* recrystallization from this solution.

2.6. Reusability of the catalyst

For this purpose, and according to the above general procedure, the model reaction for the synthesis of **4c** was selected, and it

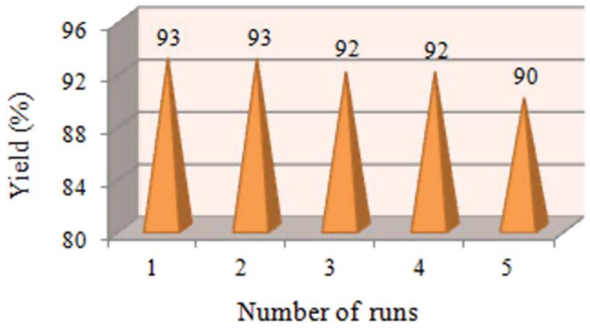

Fig. 1 The reusability of the catalyst.

was consecutively carried out over a number of cycles using the recovered catalyst under the same conditions. After the completion of each run of the reaction, the catalyst was separated easily from the reaction mixture with an external magnet and washed with hot ethanol, and it could be reused at least five times without considerable loss of catalytic activity (Fig. 1).

2.7. Spectroscopic data

9,11-Dimethyl-7-phenyl-6*H*-chromeno[3′,4′:5,6]pyrido[2,3-*d*]pyrimidine-6,8,10(9*H*,11*H*)trione (4a). White solid; yield: 0.354 g (92%); mp > 300 °C. IR (KBr) (ν_{max}/cm^{-1}): 2845, 2732, 1706, 1658, 1618, 1571, 1510, 1450, 1356, 767. ^{1}H-NMR: δ = 3.26 (s, 3H, NCH_3), 3.49 (s, 3H, NCH_3), 7.47 (d, 3H, J = 7.2 Hz, H–Ar), 7.58 (d, 2H, J = 7.2 Hz, H–Ar), 7.68 (t, 1H, J = 7.2 Hz, H–Ar), 7.75 (d, 1H, J = 8.2 Hz, H–Ar), 7.97 (t, 1H, J = 7.6 Hz, H–Ar), 8.16 (d, 1H, J = 7.6 Hz, H–Ar) ppm. ^{13}C-NMR: δ = 27.1, 29.0, 105.7, 112.5, 113.9, 117.8, 121.4, 124.6, 126.6, 127.2, 129.0, 131.3, 134.6, 135.9, 140.8, 142.9, 150.9, 157.0, 169.0, 173.1 ppm. Anal. calc. for $C_{22}H_{15}N_3O_4$ (385.38): C 68.57, H 3.92, N 10.90; found: C 68.69, H 3.82, N 10.81.

9,11-Dimethyl-7-(4-bromophenyl)-6*H*-chromeno[3′,4′:5,6]-pyrido[2,3-*d*]pyrimidine-6,8,10(9*H*,11*H*)trione (4b). White solid; yield: 0.441 g (95%); mp > 300 °C. IR (KBr) (ν_{max}/cm^{-1}): 2937, 2760, 1700, 1666, 1618, 1572, 1508, 1449, 1351, 762. ^{1}H-NMR: δ = 3.25 (s, 3H, NCH_3), 3.49 (s, 3H, NCH_3), 7.34 (d, 2H, J = 8.2 Hz, H–Ar), 7.59 (d, 1H, J = 7.8 Hz, H–Ar), 7.62 (d, 2H, J = 8.2 Hz, H–Ar), 7.65 (d, 1H, J = 8.7 Hz, H–Ar), 7.88 (t, 1H, J = 7.8 Hz, H–Ar), 8.05 (d, 1H, J = 7.8 Hz, H–Ar) ppm. ^{13}C-NMR: δ = 27.7, 29.1, 105.3, 112.4, 113.1, 117.8, 122.9, 124.6, 125.0, 127.1, 128.3, 129.2, 131.7, 138.9, 140.2, 142.9, 150.7, 157.5, 170.4, 172.9 ppm. Anal. calc. for $C_{22}H_{14}BrN_3O_4$ (464.27): C 56.92, H 3.04, N 9.05; found: C 57.05, H 3.21, N 9.15.

9,11-Dimethyl-7-(4-chlorophenyl)-6*H*-chromeno[3′,4′:5,6]-pyrido[2,3-*d*]pyrimidine-6,8,10(9*H*,11*H*)trione (4c). White solid; yield: 0.390 g (93%); mp > 300 °C. IR (KBr) (ν_{max}/cm^{-1}): 2952, 2871, 1689, 1668, 1619, 1570, 1511, 1443, 1355, 752. ^{1}H-NMR: δ = 3.27 (s, 3H, NCH_3), 3.50 (s, 3H, NCH_3), 7.45 (d, 2H, J = 8.1 Hz, H–Ar), 7.54 (d, 2H, J = 8.1 Hz, H–Ar), 7.63 (t, 1H, J = 7.5 Hz, H–Ar), 7.70 (d, 1H, J = 8.3 Hz, H–Ar), 7.92 (t, 1H, J = 7.6 Hz, H–Ar), 8.11 (d, 1H, J = 7.6 Hz, H–Ar) ppm. ^{13}C-NMR: δ = 27.1, 29.1, 105.4, 112.6, 114.0, 117.8, 124.6, 125.2, 127.4, 129.3, 131.2, 133.4, 134.1, 138.4, 140.8, 142.7, 150.9, 156.9, 168.8, 172.5 ppm. Anal. calc. for $C_{22}H_{14}ClN_3O_4$ (419.82): C 62.94, H 3.36, N 10.01; found: C 63.05, H 3.46, N 10.13.

9,11-Dimethyl-7-(4-cyanophenyl)-6*H*-chromeno[3′,4′:5,6]pyrido[2,3-*d*]pyrimidine-6,8,10(9*H*,11*H*)trione (4d). Pale yellow solid; yield: 0.394 g (96%); mp > 300 °C. IR (KBr) (ν_{max}/cm^{-1}): 2965, 2883, 2223, 1705, 1667, 1619, 1572, 1505, 1450, 1345, 759. ^{1}H-NMR: δ = 3.26 (s, 3H, NCH_3), 3.50 (s, 3H, NCH_3), 7.73 (d, 2H, J = 8.2 Hz, H–Ar), 7.76 (d, 2H, J = 8.2 Hz, H–Ar), 7.81 (d, 1H, J = 8.3 Hz, H–Ar), 8.05 (m, 2H, H–Ar), 8.21 (d, 1H, J = 7.9 Hz, H–Ar) ppm. ^{13}C-NMR: δ = 27.2, 29.1, 105.2, 110.4, 112.6, 114.5, 117.8, 119.8, 124.0, 125.0, 128.2, 129.4, 134.5, 135.3, 139.1, 140.7, 142.6, 150.9, 156.2, 169.2, 173.0 ppm. Anal. calc. for $C_{23}H_{14}N_4O_4$ (410.39): C 67.31, H 3.44, N 13.65; found: C 67.17, H 3.52, N 13.49.

9,11-Dimethyl-7-(3-hydroxyphenyl)-6*H*-chromeno[3′,4′:5,6]-pyrido[2,3-*d*]pyrimidine-6,8,10(9*H*,11*H*)trione (4e). Pale yellow solid; yield: 0.377 g (94%); mp > 300 °C. IR (KBr) (ν_{max}/cm^{-1}): 3436, 2923, 2758, 1678, 1651, 1620, 1570, 1510, 1445, 1353, 756. ^{1}H-NMR: δ = 3.25 (s, 3H, NCH_3), 3.51 (s, 3H, NCH_3), 7.52 (m, 2H, H–Ar), 7.65 (br s, 2H, H–Ar), 7.73 (t, 1H, J = 7.5 Hz, H–Ar), 7.79 (d, 1H, J = 8.2 Hz, H–Ar), 8.01 (t, 1H, J = 7.8 Hz, H–Ar), 8.21 (d, 1H, J = 7.8 Hz, H–Ar), 9.44 (s, 1H, OH) ppm. ^{13}C-NMR: δ = 27.0, 29.1, 105.5, 112.7, 113.6, 114.1, 114.5, 117.8, 124.4, 124.7, 127.3, 130.0, 133.3, 135.9, 138.4, 140.7, 143.0, 151.0, 155.9, 166.6, 169.2, 173.1 ppm. Anal. calc. for $C_{22}H_{15}N_3O_5$ (401.38): C 65.83, H 3.77, N 10.47; found: C 65.68, H 3.59, N 10.30.

9,11-Dimethyl-7-(4-methoxyphenyl)-6*H*-chromeno[3′,4′:5,6]-pyrido[2,3-*d*]pyrimidine-6,8,10(9*H*,11*H*)trione (4f). Yellow solid; yield: 0.395 g (95%); mp > 300 °C. IR (KBr) (ν_{max}/cm^{-1}): 2923, 2874, 1703, 1675, 1619, 1571, 1507, 1440, 1356, 768. ^{1}H-NMR: δ = 3.26 (s, 3H, NCH_3), 3.49 (s, 3H, NCH_3), 3.68 (s, 3H, OCH_3), 7.01 (d, 2H, J = 8.0 Hz, H–Ar), 7.27 (d, 2H, J = 8.02 Hz, H–Ar), 7.59 (t, 1H, J = 7.5 Hz, H–Ar), 7.66 (d, 1H, J = 8.2 Hz, H–Ar), 7.87 (t, 1H, J = 7.8 Hz, H–Ar), 8.06 (d, 1H, J = 7.8 Hz, H–Ar) ppm. ^{13}C-NMR: δ = 27.2, 29.1, 55.7, 105.8, 112.4, 114.0, 117.8, 123.1, 124.6, 125.2, 128.3, 129.5, 133.7, 135.3, 141.0, 142.8, 150.9, 155.9, 158.2, 167.7, 172.9 ppm. Anal. calc. for $C_{23}H_{17}N_3O_5$ (415.40): C 66.50, H 4.12, N 10.12; found: C 66.39, H 3.98, N 10.22.

9,11-Dimethyl-7-(4-methylphenyl)-6*H*-chromeno[3′,4′:5,6]-pyrido[2,3-*d*]pyrimidine-6,8,10(9*H*,11*H*)trione (4g). White solid; yield: 0.371 g (93%); mp > 300 °C. IR (KBr) (ν_{max}/cm^{-1}): 3019, 2952, 1701, 1673, 1623, 1571, 1509, 1446, 1356, 767. ^{1}H-NMR: δ = 2.24 (s, 3H, CH_3), 3.25 (s, 3H, NCH_3), 3.49 (s, 3H, NCH_3), 7.28 (br s, 4H, H–Ar), 7.60 (t, 1H, J = 7.4 Hz, H–Ar), 7.68 (d, 1H, J = 8.0 Hz, H–Ar), 7.90 (t, 1H, J = 7.0 Hz, H–Ar), 8.09 (d, 1H, J = 7.0 Hz, H–Ar) ppm. ^{13}C-NMR: δ = 21.4, 27.1, 29.4, 105.6, 113.2, 114.0, 117.8, 122.1, 124.6, 127.1, 129.3, 132.1, 133.3, 136.5, 137.2, 140.9, 142.8, 151.2, 156.0, 168.7, 172.9 ppm. Anal. calc. for $C_{23}H_{17}N_3O_4$ (399.40): C 69.17, H 4.29, N 10.52; found: C 69.35, H 4.44, N 10.38.

9,11-Dimethyl-7-(3-nitrophenyl)-6*H*-chromeno[3′,4′:5,6]pyrido[2,3-*d*]pyrimidine-6,8,10(9*H*,11*H*)trione (4h). Pale yellow solid; yield: 0.413 g (96%); mp > 300 °C. IR (KBr) (ν_{max}/cm^{-1}): 3008, 2984, 1704, 1676, 1610, 1572, 1520, 1485, 1346, 758. ^{1}H-NMR: δ = 3.27 (s, 3H, NCH_3), 3.53 (s, 3H, NCH_3), 7.69 (m, 1H, H–Ar), 7.75 (d, 1H, J = 7.6 Hz, H–Ar), 7.85 (t, 1H, J = 8.0 Hz, H–

Ar), 7.97 (m, 2H, H–Ar), 8.15 (d, 1H, $J = 7.7$ Hz, H–Ar), 8.24 (br s, 1H, H–Ar), 8.35 (d, 1H, $J = 8.1$ Hz, H–Ar) ppm. ^{13}C-NMR: $\delta =$ 27.2, 29.3, 105.2, 112.1, 113.5, 114.6, 116.1, 117.7, 124.3, 125.6, 128.4, 129.5, 137.5, 138.6, 140.9, 141.2, 142.6, 151.1, 155.4, 156.8, 168.4, 174.1 ppm. Anal. calc. for $C_{22}H_{14}N_4O_6$ (430.37): C 61.40, H 3.28, N 13.02; found: C 61.48, H 3.17, N 12.88.

3. Results and discussion

The present synthesis involved the cyclocondensation reaction of 4-aminocoumarin (**1**), 1,3-dimethylbarbituric acid (**2**), and aromatic aldehydes (**3**) for the synthesis of 9,11-dimethyl-7-aryl-6*H*-chromeno[3′,4′:5,6]pyrido[2,3-*d*]pyrimidine-6,8,10(9*H*,11*H*) triones (**4a–h**) in the presence of a catalytic amount of the PANI-Fe_3O_4@ZnO nanocomposite in aqueous media at room temperature (Scheme 1). For the first run of experiments, the PANI-Fe_3O_4@ZnO nanocomposite was prepared according to the general procedure described in the Experimental section. The XRD pattern of the synthesized nanocomposite shows

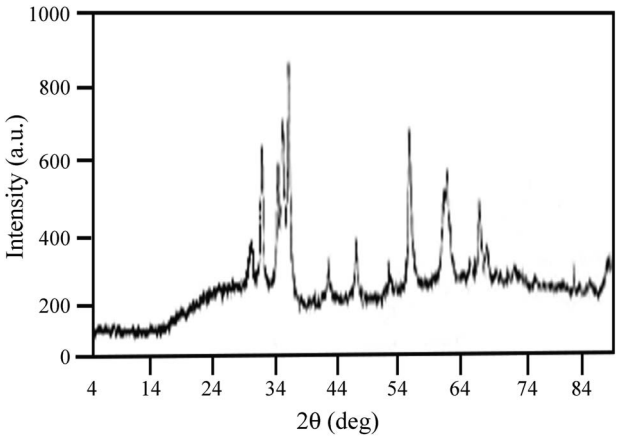

Fig. 2 The XRD pattern of the synthesized PANI-Fe_3O_4@ZnO nanocomposite.

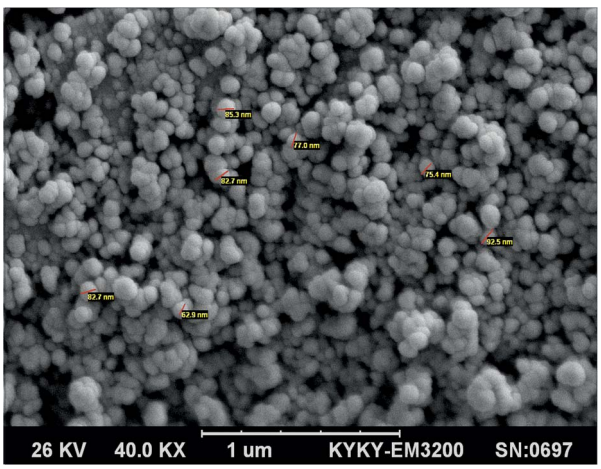

Fig. 3 An SEM image of the synthesized PANI-Fe_3O_4@ZnO nanocomposite.

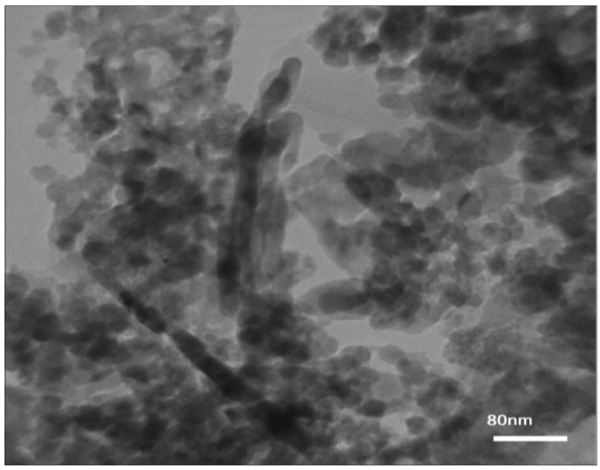

Fig. 4 A TEM image of the synthesized PANI-Fe_3O_4@ZnO nanocomposite.

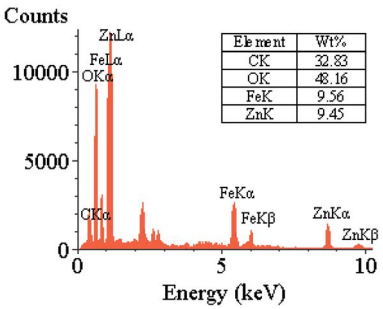

Fig. 5 The EDX spectrum of the synthesized PANI-Fe_3O_4@ZnO nanocomposite.

relatively weak and broad diffraction peaks from the lattice structure of ZnO and the spinel structure of Fe_3O_4. The broad peak at around $2\theta = 20°$ is ascribed to periodic parallel and perpendicular PANI chains in the semi-crystalline structure (Fig. 2). In the XRD pattern, the peak intensities of ZnO are stronger than those of Fe_3O_4, confirming the ZnO shell of the composite.

SEM (Fig. 3) and TEM (Fig. 4) imaging of the catalyst show that the microspheres of the PANI-Fe_3O_4@ZnO nanocomposite have an average diameter of about 75 nm and typical core–shell structure with uniform spherical morphology in which ZnO nanoparticles are dispersed uniformly around PANI.

The EDX analysis results reveal the presence of C, O, Fe, and Zn elements in the structure of the nanocomposite (Fig. 5).

In a typical experimental procedure, the reaction between 4-aminocoumarin (**1**), 1,3-dimethylbarbituric acid (**2**), and 4-chlorobenzaldehyde (**3c**) was chosen and investigated under various reaction conditions (Scheme 2 and Table 1). First, we studied the model reaction in refluxing water without any catalyst. The reaction was incomplete, with a yield of 61% even after 7 h (Table 1, entry 1). Next, we studied the use of various catalysts, including *p*-TsOH, DAHP, commercial Fe_3O_4 NPs (≤50 nm), and ZnO NPs (≤40 nm), in comparison to the PANI-

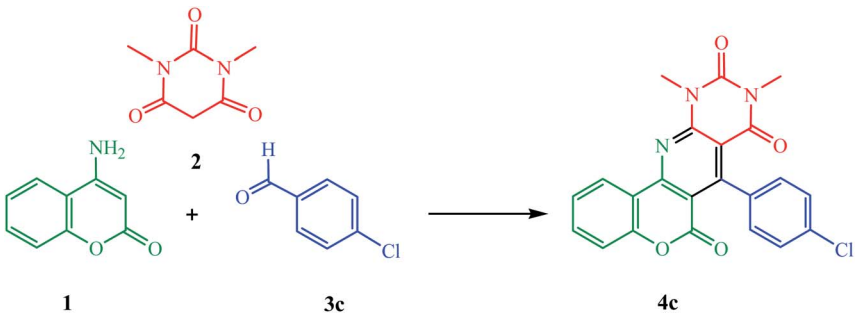

Scheme 2 The synthesis of 9,11-dimethyl-7-(4-chlorophenyl)-6*H*-chromeno[3′,4′:5,6]pyrido[2,3-*d*]pyrimidine-6,8,10(9*H*,11*H*)trione (**4c**).

Table 1 The synthesis of 9,11-dimethyl-7-(4-chlorophenyl)-6*H*-chromeno[3′,4′:5,6]pyrido[2,3-*d*]pyrimidine-6,8,10(9*H*,11*H*)trione (**4c**) under various reaction conditions

Entry	Catalyst	Solvent	Temp. (°C)	Time (h)	Yield[d,e] (%)
1	None	H_2O	Reflux	7	61
2	*p*-TsOH[a] (0.03 g)	H_2O	r.t.	5	84
3	DAHP[b] (0.03 g)	H_2O	r.t.	7	79
4	ZnO NPs (0.03 g)	H_2O	r.t.	6	86
5	Fe_3O_4 MNPs (0.03 g)	H_2O	r.t.	6	88
6	PANI-Fe_3O_4@ZnO (0.02 g)	H_2O	r.t.	6	72
7	PANI-Fe_3O_4@ZnO (0.03 g)	H_2O	r.t.	5	93
8	PANI-Fe_3O_4@ZnO (0.04 g)	H_2O	r.t.	5	93
9	PANI-Fe_3O_4@ZnO (0.03 g)	H_2O	Reflux	3	94
10	PANI-Fe_3O_4@ZnO (0.02 g)	EtOH	r.t.	2.5	71
11	PANI-Fe_3O_4@ZnO (0.02 g)	CH_3CN	r.t.	3	63
12	PANI-Fe_3O_4@ZnO (0.02 g)	CH_2Cl_2	r.t.	3	45
13	PANI-Fe_3O_4@ZnO (0.02 g)	DMF[c]	r.t.	2	76

[a] *p*-TsOH: *p*-toluenesulfonic acid. [b] DAHP: diammonium hydrogen phosphate. [c] DMF: dimethylformamide. [d] Isolated yield. [e] Reaction conditions: a mixture of 4-aminocoumarin (**1**, 1 mmol), 1,3-dimethylbarbituric acid (**2**, 1 mmol), and 4-chlorobenzaldehyde (**3c**, 1 mmol) was stirred under various reaction conditions.

Fe_3O_4@ZnO nanocomposite for the synthesis of the desired product **4c**. Among these, the PANI-Fe_3O_4@ZnO nanocomposite (0.03 g) was found to be the superior catalyst (Table 1, entries 2–8). The effect of the reaction temperature was also examined. It is noteworthy that there was no distinct difference in the yield of this conversion under reflux heating; only a reduction in the reaction time was observed (Table 1, entries 7 and 9). To prove the effective involvement of water as a reaction media, we carried out the above reaction in several solvents, including EtOH, CH_3CN, CH_2Cl_2, and DMF. The results showed that the highest yield (93%) was obtained in the presence of water (Table 1, entries 7 and 9–13).

Various aromatic aldehydes were condensed with 4-aminocoumarin and 1,3-dimethylbarbituric acid under the optimized reaction conditions to provide the corresponding products **4a–h** in high yields (Table 2). It is noticeable that the aromatic ring substituent did not produce any special effects in terms of the yields under these reaction conditions. This may be due to the speed of the first step of the reaction in the formation of the alkene. The structures of compounds **4a–h** were confirmed *via* IR, ^{1}H NMR and ^{13}C NMR spectroscopic studies, and also *via* elemental analyses. Spectroscopic data are given in the Experimental section. The synthesized catalyst was fully characterized *via* XRD, SEM, TEM, and EDX techniques.

A suggested mechanism for the reaction is outlined in Scheme 3. Initially, the PANI-Fe_3O_4@ZnO nanocomposite is involved in the formation of the alkene (**7**) *via* Knoevenagel condensation between 1,3-dimethylbarbituric acid (**2**) and the aromatic aldehyde (**3**), *via* intermediates **5** and **6**. Afterward, 4-aminocoumarin (**1**) is added to the alkene (**7**) generating the Michael adduct (**8**), which undergoes intermolecular cyclization and subsequent aromatization to produce the product (**4**). In order to demonstrate the proposed mechanism, we tried to divide the model reaction into two separate steps. In the first step, in the absence of 4-aminocoumarin (**1**), the formation of the alkene **7c** occurred from the reaction between 1,3-dimethylbarbituric acid (**2**) and 4-chlorobenzaldehyde (**3c**). When we used the preformed alkene **7c** in the reaction with 4-aminocoumarin (**1**) in a second step, it was shown that the product **4c** resulted. The crude product from the first step (the alkene **7c**) without further purification was isolated and used as a control spot in TLC testing of the three-component reaction. It was found that in the three-component reaction, alkene **7c** as a first intermediate product is formed on the TLC plate about 0.5 hour

Table 2 The PANI-Fe_3O_4@ZnO nanocomposite catalyzed synthesis of the 9,11-dimethyl-7-aryl-6*H*-chromeno[3′,4′:5,6]pyrido[2,3-*d*]pyrimidine-6,8,10(9*H*,11*H*)triones **4a–h**

Product	Ar	Time (h)	Yield[a,b] (%)	Mp (°C)
4a	C_6H_5	5	92	>300
4b	4-Br–C_6H_4	5	95	>300
4c	4-Cl–C_6H_4	5.5	93	>300
4d	4-CN–C_6H_4	5.5	96	>300
4e	3-OH–C_6H_4	5	94	>300
4f	4-OCH_3–C_6H_4	7	95	>300
4g	4-CH_3–C_6H_4	6.5	93	>300
4h	3-NO_2–C_6H_4	6	96	>300

[a] Yield refers to the pure isolated product characterized *via* IR, ^{1}H NMR and ^{13}C NMR spectral data and *via* elemental analyses. [b] Reaction conditions: a mixture of 4-aminocoumarin (**1**, 1 mmol), 1,3-dimethylbarbituric acid (**2**, 1 mmol), aromatic aldehyde (**3**, 1 mmol), and PANI-Fe_3O_4@ZnO nanocomposite (0.03 g) in H_2O (3 mL) was stirred at ambient temperature for an appropriate time.

after the start of the reaction, which is presumed to come from the reaction of 1,3-dimethylbarbituric acid (**2**) with 4-chlorobenzaldehyde (**3c**), and then the final product is obtained from the reaction of this intermediate with 4-aminocoumarin (**1**) after a specific period of time.

4. Conclusions

In summary, a PANI-Fe_3O_4@ZnO nanocomposite was synthesized through a new strategy, characterized and applied as a suitable heterogenous catalyst for the environmentally friendly and economic synthesis of 9,11-dimethyl-7-aryl-6*H*-chromeno[3′,4′:5,6]pyrido[2,3-*d*]pyrimidine-6,8,10(9*H*,11*H*)triones *via* cyclocondensation reactions between 4-aminocoumarin, 1,3-dimethylbarbituric acid, and aromatic aldehydes. The appearance of relevant absorption peaks in the XRD pattern confirmed the successful synthesis of the nanocatalyst. In the EDX spectrum of the nanocatalyst, the expected elements were displayed. The average size and morphology of the nanocatalyst were determined from SEM and TEM images. The structures of compounds **4a–h** were fully confirmed *via* IR, ^{1}H NMR and ^{13}C NMR spectroscopic studies, and also from elemental analyses. High yields of products, the use of a green solvent, the easy work-up procedure, the short reaction times, and the easily separable catalyst are the main advantages of this protocol. The magnetically recovered catalyst could be reused appropriately many times with suitable catalyst activity.

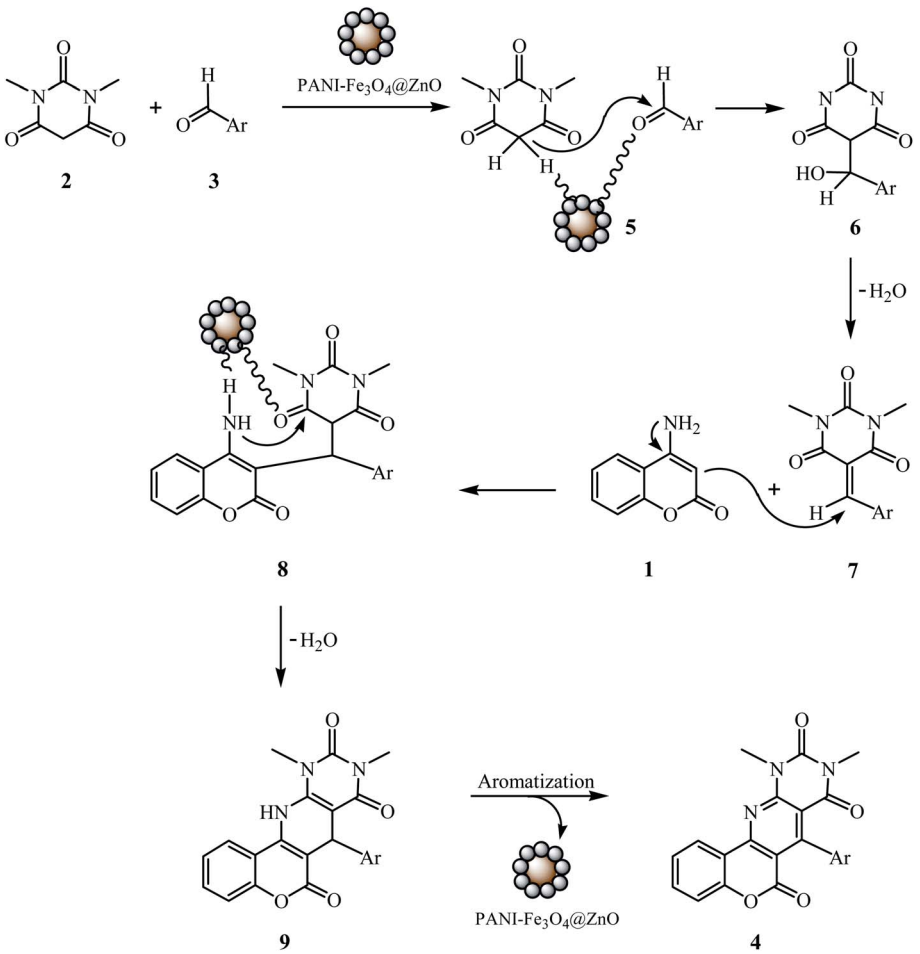

Scheme 3 The proposed mechanism for the formation of **4**.

Conflicts of interest

There are no conflicts to declare.

Acknowledgements

Shahrzad Abdolmohammadi is grateful to the Research Council of East Tehran Branch, Islamic Azad University for financial support.

References

1 I. Horvath and P. Anastas, *Chem. Rev.*, 2007, **107**, 2167–2168.
2 S. L. Schreiber, *Nature*, 2009, **457**, 153–154.
3 J. Zhu and H. Bienayme, *Multicomponent Reactions*, Wiley-VCH, Weinheim, 2005.
4 B. M. Trost, *Acc. Chem. Res.*, 2002, **35**, 695–705.
5 P. A. Wender, V. A. Verma, T. J. Paxton and T. H. Pillow, *Acc. Chem. Res.*, 2008, **41**, 40–49.
6 S. Farshbaf, L. Sreerama, T. Khodayari and E. Vessally, *Chem. Rev. Lett.*, 2018, **1**, 56–67.
7 F. Behmagham, Z. Asadi and Y. J. Sadeghi, *Chem. Rev. Lett.*, 2018, **1**, 68–76.
8 S. Zhi, X. Ma and W. Zhang, *Org. Biomol. Chem.*, 2019, **17**, 7632–7650.
9 H. G. O. Alvim, J. R. Correa, J. A. F. Assumpção, W. A. da Silva, M. O. Rodrigues, J. L. de Macedo, M. Fioramonte, F. C. Gozzo, C. C. Gatto and B. A. D. Neto, *J. Org. Chem.*, 2018, **83**, 4044–4053.
10 A. V. Vasco, Y. Méndez, A. Porzel, J. Balbach, L. A. Wessjohann and D. G. Rivera, *Bioconjugate Chem.*, 2019, **30**, 253–259.
11 L. S. da Silveira Pinto, M. R. C. Couri and M. V. N. de Souza, *Curr. Org. Synth.*, 2018, **15**, 21–37.
12 A. C. Boukis, K. Reiter, M. Frölich, D. Hofheinz and M. A. R. Meier, *Nat. Commun.*, 2018, **9**, 1439.
13 M. Nikpassand and L. ZareFekri, *Chem. Rev. Lett.*, 2019, **2**, 7–12.
14 F. Valinia, N. Shojaei and P. Ojaghloo, *Chem. Rev. Lett.*, 2019, **2**, 90–97.
15 E. Jafari, P. Farajzadeh, N. Akbari and A. Karbakhshzadeh, *Chem. Rev. Lett.*, 2019, **2**, 123–129.
16 Y. M. Huh, Y. W. Jun, H. T. Song, S. Kim, J. S. Choi, J. H. Lee, S. Yoon, K. S. Kim, J. S. Shin, J. S. Suh and J. Cheon, *J. Am. Chem. Soc.*, 2005, **127**, 12387–12391.
17 P. Sharma, S. Rana, K. C. Barick, C. Kumar, H. G. Salunked and P. A. Hassan, *New J. Chem.*, 2014, **38**, 5500–5508.
18 J. Deng, L. P. Mo, F. Y. Zhao, L. L. Hou, L. Yang and Z. H. Zhang, *Green Chem.*, 2011, **13**, 2576–2584.
19 R. K. Sharma, S. Dutta, S. Sharma, R. Zboril, R. S. Varma and M. B. Gawande, *Green Chem.*, 2016, **18**, 3184–3209.
20 L. Javadian and J. Safari, *Iran. J. Catal.*, 2016, **6**, 57–64.
21 R. Gupta, M. Yadav, R. Gaur, G. Arora, P. Rana, P. Yadav, A. Adholeya and R. K. Sharma, *ACS Omega*, 2019, **4**, 21529–21539.
22 S. Fakheri-Vayeghan, S. Abdolmohammadi and R. Kia-Kojoori, *Z. Naturforsch., B: Chem. Sci.*, 2018, **73**, 545–551.
23 D. Girija, H. S. B. Naik, B. V. Kumar, C. N. Sudhamani and K. N. Harish, *Arabian J. Chem.*, 2019, **12**, 420–428.
24 N. M. Dimitrijevic, S. Tepavcevic, Y. Liu, T. Rajh, S. C. Silver and D. M. Tiede, *J. Phys. Chem. C*, 2013, **117**, 15540–15544.
25 C. W. Peng, K. C. Chang, C. J. Weng, M. C. Lai, C. H. Hsu, S. C. Hsu, Y. Y. Hsu, W. I. Hung, Y. Wei and J. M. Yeh, *Electrochim. Acta*, 2013, **95**, 192–199.
26 X. Wang, Y. Shen, A. Xie, L. Qiu, S. Li and Y. Wang, *J. Mater. Chem.*, 2011, **21**, 9641–9646.
27 L. Liang, J. Liu, C. F. W. Indisch Jr, G. J. Exarhos and Y. Lin, *Angew. Chem., Int. Ed.*, 2002, **41**, 3665–3668.
28 S. Xiong, Q. Wang and H. Xia, *Synth. Met.*, 2004, **146**, 37–42.
29 D. W. Hatchett and M. Josowicz, *Chem. Rev.*, 2008, **108**, 746–769.
30 R. Pratap and V. J. Ram, *Chem. Rev.*, 2014, **114**, 10476–10526.
31 M. Kidwai, S. Saxena, M. K. Rahman Khan and S. S. Thukral, *Bioorg. Med. Chem. Lett.*, 2005, **15**, 4295–4298.
32 R. R. Kumar, S. Perumal, P. Senthilkumar, P. Yogeeswari and D. Sriram, *Bioorg. Med. Chem. Lett.*, 2007, **17**, 6459–6462.
33 I. O. Donkor, C. L. Klein, L. Liang, N. Zhu, E. Bradley and A. M. Clark, *J. Pharm. Sci.*, 1995, **84**, 661–664.
34 M. M. Khafagy, A. H. Abd el-Wahab, F. A. Eid and A. M. el-Agrody, *Farmaco*, 2002, **57**, 715–722.
35 L. Alvey, S. Prado, V. Huteau, B. Saint-Joanis, S. Michel, M. Koch, S. T. Cole, F. Tillequin and Y. L. Janin, *Bioorg. Med. Chem.*, 2008, **16**, 8264–8272.
36 A. H. Bedair, N. A. El-Hady, A. El-Latif, A. H. Fakery and A. M. El-Agrody, *Farmaco*, 2000, **55**, 708–714.
37 M. Mladenović, M. Mihailović, D. Bogojević, S. Matić, N. Nićiforović, V. Mihailović, N. Vuković, S. Sukdolak and S. I. Solujić, *Int. J. Mol. Sci.*, 2011, **12**, 2822–2841.
38 T. Symeonidis, M. Chamilos, D. J. Hadjipavlou-Litina, M. Kallitsakis and K. E. Litinas, *Bioorg. Med. Chem. Lett.*, 2009, **19**, 1139–1142.
39 H. Gourdeau, L. Leblond, B. Hamelin, C. Desputeau, K. Dong, I. Kianicka, D. Custeau, C. Boudreau, L. Geerts, S. X. Cai, J. Drewe, D. Labrecque, S. Kasibhatla and B. Tseng, *Mol. Cancer Ther.*, 2004, **3**, 1375–1384.
40 V. K. Tandon, M. Vaish, S. Jain, D. S. Bhakuni and R. C. Srimal, *Indian J. Pharm. Sci.*, 1991, **53**, 22–23.
41 J. L. Wang, D. Liu, Z. J. Zhang, S. Shan, X. Han, S. M. Srinivasula, C. M. Croce, E. S. Alnemri and Z. Huang, *Proc. Natl. Acad. Sci. U. S. A.*, 2000, **97**, 7124–7129.
42 F. Cheng, A. Ishikawa, Y. Ono, T. Arrheniusa and A. Nadzana, *Bioorg. Med. Chem. Lett.*, 2003, **13**, 3647–3650.
43 D. Grée, S. Vorin, V. L. Manthati, F. Caijo, G. Viault, F. Manero, P. Juin and R. Grée, *Tetrahedron Lett.*, 2008, **49**, 3276–3278.
44 W. Kemnitzer, S. Jiang, H. Zhang, S. Kasibhatla, C. Crogan-Grundy, C. Blais, G. Attardo, R. Denis, S. Lamothe, H. Gourdeau, B. Tseng, J. Drewe and X. Cai, *Bioorg. Med. Chem. Lett.*, 2008, **18**, 5571–5575.

45 M. Longobardi, A. Bargagna, E. Mariani, P. Schenone, S. Vitagliano, L. Stella, A. Di Sarno and E. Marmo, *Farmaco*, 1990, **45**, 399–401.
46 T. A. Bayer, S. Schäfer, H. Breyhan, O. Wirths, C. Treiber and G. Multhaup, *Clin. Neuropathol.*, 2006, **25**, 163–171.
47 G. D. Henry, *Tetrahedron*, 2004, **60**, 6043–6061.
48 S. Abdolmohammadi, *Comb. Chem. High Throughput Screening*, 2018, **21**, 594–601.
49 S. Abdolmohammadi, B. Mirza and E. Vessally, *RSC Adv.*, 2019, **9**, 41868–41876.
50 S. Abdolmohammadi, S. R. Rasouli Nasrabadi, M. R. Dabiri and S. M. Banihashemi Jozdani, *Appl. Organomet. Chem.*, 2020, **34**, e5462.